An Algebraic Approach to Practical and Scalable Overlay Network Monitoring

Yan Chen
Department of Computer Science
Northwestern University
ychen@cs.northwestern.edu

David Bindel   Hanhee Song   Randy H. Katz
Division of Computer Science
University of California at Berkeley
(dbindel@cs, coolcoon@uclink, randy@cs).berkeley.edu

Overlay network monitoring enables distributed Internet applications to detect and recover from path outages and periods of degraded performance within seconds. For an overlay network with n end hosts, existing systems either require $O(n^2)$ measurements, and thus lack scalability, or can only estimate the latency but not congestion or failures. Our earlier extended abstract [1] briefly proposes an algebraic approach that selectively monitors k linearly independent paths that can fully describe all the $O(n^2)$ paths. The loss rates and latency of these k paths can be used to estimate the loss rates and latency of all other paths. Our scheme only assumes knowledge of the underlying IP topology, with links dynamically varying between lossy and normal.

In this paper, we improve, implement and extensively evaluate such a monitoring system. We further make the following contributions: i) scalability analysis indicating that for reasonably large n (*e.g.*, 100), the growth of k is bounded as $O(n \log n)$, ii) efficient adaptation algorithms for topology changes, such as the addition or removal of end hosts and routing changes, iii) measurement load balancing schemes, and iv) topology measurement error handling. Both simulation and Internet experiments demonstrate we obtain highly accurate path loss rate estimation while adapting to topology changes within seconds and handling topology errors.

Categories and Subject Descriptors

C.2.3 [**Network Operations**]: Network monitoring

General Terms

Algorithms, Measurement

Keywords

Overlay, Network measurement and monitoring, Numerical linear algebra, Scalability, Dynamics, Load balancing

1. INTRODUCTION

The rigidity of the Internet architecture makes it extremely difficult to deploy innovative disruptive technologies in the core. This has led to extensive research into overlay and peer-to-peer systems, such as overlay routing and location, application-level multicast, and peer-to-peer file sharing. These systems flexibly choose their communication paths and targets, and thus can benefit from estimation of end-to-end network distances (*e.g.*, latency and loss rate).

Accurate loss rate monitoring systems can detect path outages and periods of degraded performance within seconds. They facilitate management of distributed systems such as virtual private networks (VPM) and content distribution networks; and they are useful for building adaptive overlay applications, such as the streaming media framework demonstrated in [2].

Thus it is desirable to have a scalable overlay loss rate monitoring system which is accurate and incrementally deployable. However, existing network distance estimation systems are insufficient for this end. These existing systems can be categorized as *general metric* systems [3] and *latency-only* systems [4, 5, 6, 7]. Systems in the former category can measure any metric, but require $O(n^2)$ measurements where n is the number of end hosts, and thus lack scalability. On the other hand, the latency estimation systems are scalable, but cannot provide accurate congestion/failure detection (see Sec. 2).

We formulate the problem as follows: consider an overlay network of n end hosts; we define a path to be a routing path between a pair of end hosts, and a link to be an IP link between routers. A path is a concatenation of links. There are $O(n^2)$ paths among the n end hosts, and we wish to select a minimal subset of paths to monitor so that the loss rates and latencies of all other paths can be inferred.

In an earlier extended abstract [1], we sketched the idea of a tomography-based overlay monitoring system (TOM) in which we selectively monitor a *basis set* of k paths. Any end-to-end path can be written as a unique linear combination of paths in the basis set. Consequently, by monitoring loss rates for the paths in the basis set, we infer loss rates for all end-to-end paths. This can also be extended to other additive metrics, such as latency. The end-to-end path loss rates can be computed even when the paths contain *unidentifiable links* for which loss rates cannot be computed.

In [1], we only briefly introduce the basic formulation and model. The following questions remain:

- How scalable is the system? In other words, how will k grow as a function of n? It is our conjecture that for reasonably large n (say 100), $k = O(n \log n)$ [1].

- In an overlay network, end hosts frequently join/leave the overlay and routing changes occur from time to time. How can the system adapt to these efficiently?
- How should the system distribute the measurement load among end hosts to improve scalability?
- How can the system maintain accuracy when there are topology measurement errors?
- How does TOM perform under various topologies and loss conditions, and in the real Internet?

To address these issues, in this paper, we make the following contributions.

- We show that k does grow as $O(n \log n)$ through linear regression tests on various synthetic and real topologies. We also provide some explanation based on the Internet topology and the AS hierarchy.
- We design incremental algorithms for path addition and deletion which only cost $O(k^2)$ time, instead of the $O(n^2 k^2)$ time cost to reinitialize the system.
- We propose randomized schemes for measurement load balancing.
- We design effective schemes to handle topology measurement errors.
- We evaluate TOM through extensive simulations, and further validate our results through Internet experiments.

In both simulations and PlanetLab experiments, we estimate path loss rates with high accuracy using $O(n \log n)$ measurements. For the PlanetLab experiments, the average absolute error of loss rate estimation is only 0.0027, and the average error factor is 1.1, even though about 10% of the paths have incomplete or nonexistent routing information. The average setup (monitoring path selection) time is 0.75 second, and the online update of the loss rates for all 2550 paths takes only 0.16 second. In addition, we adapt to topology changes within seconds without sacrificing accuracy. The measurement load balancing reduces the load variation and the maximum vs. mean load ratio significantly, by up to a factor of 7.3.

The rest of the paper is organized as follows. We survey related work in Sec. 2, describe our model and basic static algorithms in Sec. 3, and evaluate scalability in Sec. 4. We extend the algorithms to adapt to topology changes in Sec. 5, and to handle overload and topology measurement errors in Sec. 6. The methodology and results of our simulations are described in Sec. 7, and those of our Internet experiments are presented in Sec. 8. Finally, we conclude in Sec. 9.

2. RELATED WORK

There are many existing scalable end-to-end latency estimation schemes, which can be broadly classified into clustering-based [6, 7] and coordinate-based systems [4, 5]. Clustering-based systems cluster end hosts based on their network proximity or latency similarity under normal conditions, then choose the centroid of each cluster as the monitor. But a monitor and other members of the same cluster often take different routes to remote hosts. So the monitor cannot detect congestion for its members. Similarly, the coordinates assigned to each end host in the coordinate-based approaches cannot embed any congestion/failure information.

Network tomography has been well studied ([8] provides a good survey). Most tomography systems assume limited measurements are available (often in a multicast tree-like structure), and try to infer link characteristics [9, 10] or shared congestion [11] in the middle of the network. However, the problem is under-constrained: there exist *uniden-*
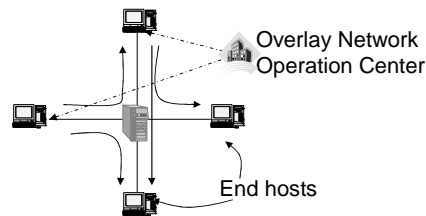

Figure 1: Architecture of a TOM system.

tifiable links [9] with properties that cannot be uniquely determined. In contrast, we are not concerned about the characteristics of *individual* links, and we do not restrict the paths we measure.

Shavitt, *et al.* also use algebraic tools to compute distances that are not explicitly measured [12]. Given certain "Tracer" stations deployed and some direct measurements among the Tracers, they search for path or path segments whose loss rates can be inferred from these measurements. Thus their focus is not on Tracer/path selection.

Recently, Ozmutlu, *et al.* selected a minimal subset of paths to cover all links for monitoring, assuming link-by-link latency is available via end-to-end measurement [13]. But the link-by-link latency obtained from traceroute is often inaccurate. And their approach is not applicable for loss rate because it is difficult to estimate link-by-link loss rates from end-to-end measurement. A similar approach was taken for selecting paths to measure overlay network [14]. The minimal set cover selected can only gives *bounds* for metrics like latency, and there is no guarantee as to how far the bounds are from the real values.

Furthermore, none of the existing work examines topology change, topology measurement errors, or measurement load balancing problems.

3. MODEL AND BASIC ALGORITHMS

3.1 Algebraic Model

Suppose there are n end hosts that belong to a single or confederated overlay network(s). They cooperate to share an overlay monitoring service, and are instrumented by a central authority (*e.g.*, an overlay network operation center (ONOC)) to measure the routing topology and path loss rates as needed [1]. For simplicity, we usually assume symmetric routing and undirected links in this paper. However, our techniques work without change for asymmetric routing, as evidenced in the PlanetLab experiments. Fig. 1 shows a sample overlay network with four links and four end hosts; six possible paths connect the end hosts. The end hosts measure the topology and report to the ONOC, which selects four paths and instruments two of the end hosts to measure the loss rates of those paths. The end hosts periodically report the measured loss rates to the ONOC. Then the ONOC infers the loss rates of every link, and consequently the loss rates of the other two paths. Applications can query the ONOC for the loss rate of any path, or they can set up triggers to receive alerts when the loss rates of paths of interest exceed a certain threshold [2].

We now introduce an algebraic model which applies to any network topology. Suppose an overlay network spans s IP links. We represent a path by a column vector $v \in$

---

[1]As part of the future work, we will investigate techniques to distribute the work of the central authority.

Symbols	Meanings
M	total number of nodes
N	number of end hosts
n	number of end hosts on the overlay
$r = O(n^2)$	number of end-to-end paths
s	# of IP links that the overlay spans on
t	number of identifiable links
$G \in \{0,1\}^{r \times s}$	original path matrix
$\bar{G} \in \{0,1\}^{k \times s}$	reduced path matrix
$k \leq s$	rank of G
l_i	loss rate on ith link
p_i	loss rate on ith measurement path
x_i	$\log(1 - l_i)$
b_i	$\log(1 - p_i)$
v	vector in $\{0,1\}^s$ (represents path)
p	loss rate along a path
$\mathcal{N}(G)$	null space of G
$\mathcal{R}(G^T)$	row(path) space of G ($==$ range(G^T))

Table 1: Table of notations

$\{0,1\}^s$, where the jth entry v_j is one if link j is part of the path, and zero otherwise. Suppose link j drops packets with probability l_j; then the loss rate p of a path represented by v is given by

$$1 - p = \prod_{j=1}^{s} (1 - l_j)^{v_j} \qquad (1)$$

Equation (1) assumes that packet loss is independent among links. Caceres *et al.* argue that the diversity of traffic and links makes large and long-lasting spatial link loss dependence unlikely in a real network such as the Internet [15]. Furthermore, the introduction of Random Early Detection (RED) [16] policies in routers will help break such dependence. In addition to [15], formula (1) has also been proven useful in many other link/path loss inference works [10, 9, 17, 14]. Our Internet experiments also show that the link loss dependence has little effect on the accuracy of (1).

We take logarithms on both sides of (1). Then by defining a column vector $x \in \mathbb{R}^s$ with elements $x_j = \log(1 - l_j)$, and writing v^T for the transpose of the column vector v, we can rewrite (1) as follows:

$$\log(1 - p) = \sum_{j=1}^{s} v_j \log(1 - l_j) = \sum_{j=1}^{s} v_j x_j = v^T x \qquad (2)$$

There are $r = O(n^2)$ paths in the overlay network, and thus there are r linear equations of the form (2). Putting them together, we form a rectangular matrix $G \in \{0,1\}^{r \times s}$. Each row of G represents a path in the network: $G_{ij} = 1$ when path i contains link j, and $G_{ij} = 0$ otherwise. Let p_i be the end-to-end loss rate of the ith path, and let $b \in \mathbb{R}^r$ be a column vector with elements $b_i = \log(1 - p_i)$. Then we write the r equations in form (2) as

$$Gx = b \qquad (3)$$

Normally, the number of paths r is much larger than the number of links s (see Fig. 2(a)). This suggests that we could select s paths to monitor, use those measurements to compute the link loss rate variables x, and infer the loss rates of the other paths from (3).

However, in general, G is rank deficient: *i.e.*, $k = \text{rank}(G)$ and $k < s$. If G is rank deficient, we will be unable to deter-
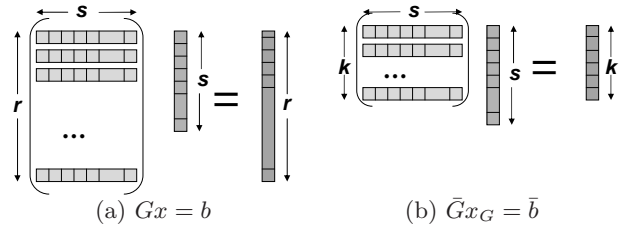

(a) $Gx = b$ (b) $\bar{G}x_G = \bar{b}$

Figure 2: Matrix size representations.

mine the loss rate of some links from (3). These links are also called *unidentifiable* in network tomography literature [9].
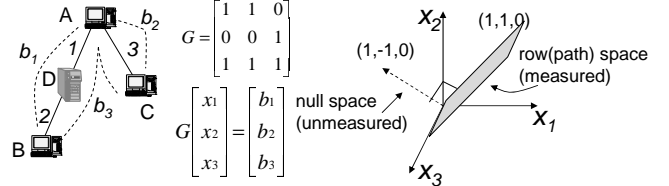

Figure 3: Sample overlay network.

Fig. 3 illustrates how rank deficiency can occur. There are three end hosts (A, B and C) on the overlay, three links (1, 2 and 3) and three paths between the end hosts. We cannot uniquely solve x_1 and x_2 because links 1 and 2 always appear together. We know their sum, but not their difference.

Fig. 3 illustrates the geometry of the linear system, with each variable x_i as a dimension. The vectors $\{\alpha \begin{bmatrix} 1 & -1 & 0 \end{bmatrix}^T\}$ comprise $\mathcal{N}(G)$, the *null space* of G. No information about the loss rates for these vectors is given by (3). Meanwhile, there is an orthogonal *row(path) space* of G, $\mathcal{R}(G^T)$, which for this example is a plane $\{\alpha \begin{bmatrix} 1 & 1 & 0 \end{bmatrix}^T + \beta \begin{bmatrix} 0 & 0 & 1 \end{bmatrix}^T\}$. Unlike the null space, the loss rate of any vector on the row space can be uniquely determined by (3).

To separate the identifiable and unidentifiable components of x, we decompose x into $x = x_G + x_N$, where $x_G \in \mathcal{R}(G^T)$ is its projection on the row space and and $x_N \in \mathcal{N}(G)$ is its projection on the null space (*i.e.*, $Gx_N = 0$). The decomposition of $\begin{bmatrix} x_1 & x_2 & x_3 \end{bmatrix}^T$ for the sample overlay is shown below.

$$x_G = \frac{(x_1 + x_2)}{2} \begin{bmatrix} 1 \\ 1 \\ 0 \end{bmatrix} + x_3 \begin{bmatrix} 0 \\ 0 \\ 1 \end{bmatrix} = \begin{bmatrix} b_1/2 \\ b_1/2 \\ b_2 \end{bmatrix} \qquad (4)$$

$$x_N = \frac{(x_1 - x_2)}{2} \begin{bmatrix} 1 \\ -1 \\ 0 \end{bmatrix} \qquad (5)$$

Thus the vector x_G can be uniquely identified, and contains all the information we can know from (3) and the path measurements. The intuition of our scheme is illustrated through *virtual links* in [1].

Because x_G lies in the k-dimensional space $\mathcal{R}(G^T)$, only k independent equations of the r equations in (3) are needed to uniquely identify x_G. We measure these k paths to compute x_G. Since $b = Gx = Gx_G + Gx_N = Gx_G$, we can compute all elements of b from x_G, and thus obtain the loss rate of all other paths. Next, we present more detailed algorithms.

3.2 Basic Static Algorithms

The basic algorithms involve two steps. First, we select a basis set of k paths to monitor. Such selection only needs to

be done once at setup. Then, based on continuous monitoring of the selected paths, we calculate and update the loss rates of all other paths.

3.2.1 Measurement Paths Selection

To select k linearly independent paths from G, we use standard rank-revealing decomposition techniques [18], and obtain a reduced system:

$$\bar{G}x_G = \bar{b} \tag{6}$$

where $\bar{G} \in \mathbb{R}^{k \times s}$ and $\bar{b} \in \mathbb{R}^k$ consist of k rows of G and b, respectively. The equation is illustrated in Fig. 2(b) (compared with $Gx = b$).

As shown below, our algorithm is a variant of the QR decomposition with column pivoting [18, p.223]. It incrementally builds a decomposition $\bar{G}^T = QR$, where $Q \in \mathbb{R}^{s \times k}$ is a matrix with orthonormal columns and $R \in \mathbb{R}^{k \times k}$ is upper triangular.

---

procedure SelectPath(G)
1 **for** *every row(path) v in G* **do**
2     $\hat{R}_{12} = R^{-T}\bar{G}v^T = Q^Tv^T$
3     $\hat{R}_{22} = \|v\|^2 - \|\hat{R}_{12}\|^2$
4   **if** $\hat{R}_{22} \neq 0$ **then**
5   Select v as a measurement path
6   Update $R = \begin{bmatrix} R & \hat{R}_{12} \\ 0 & \hat{R}_{22} \end{bmatrix}$ and $\bar{G} = \begin{bmatrix} \bar{G} \\ v \end{bmatrix}$
    end
end

Algorithm 1: Path (row) selection algorithm

In general, the G matrix is very sparse; that is, there are only a few nonzeros per row. We leverage this property for speedup. We further use optimized routines from the LAPACK library [19] to implement Algorithm 1 so that it inspects several rows at a time. The complexity of Algorithm 1 is $O(rk^2)$, and the constant in the bound is modest. The memory cost is roughly $k^2/2$ single-precision floating point numbers for storing the R factor. Notice that the path selection only needs to be executed once for initial setup.

3.2.2 Path Loss Rate Calculations

To compute the path loss rates, we must find a solution to the underdetermined linear system $\bar{G}x_G = \bar{b}$. The vector $\bar{b}$ comes from measurements of the paths. Zhang *et al.* report that path loss rates remain operationally stable in the time scale of an hour [20], so these measurements need not be taken simultaneously.

Given measured values for $\bar{b}$, we compute a solution x_G using the QR decomposition we constructed during measurement path selection [18, 21]. We choose the unique solution x_G with minimum possible norm by imposing the constraint $x_G = \bar{G}^Ty$ where $y = R^{-1}R^{-T}\bar{b}$. Once we have x_G, we can compute $b = Gx_G$, and from there infer the loss rates of the unmeasured paths. The complexity for this step is only $O(k^2)$. Thus we can update loss rate estimates online, as verified in Sec. 7.4 and 8.2.

4. SCALABILITY ANALYSIS

An overlay monitoring system is scalable only when the size of the basis set, k, grows relatively slowly as a function of n. Given that the Internet has moderate hierarchical structure [22, 23], we proved that the number of end hosts is no less than half of the total number of nodes in the Internet. Furthermore, we proved that when all the end hosts are on the overlay network, $k = O(n)$ [1].

But what about if only a small fraction of the end hosts are on the overlay? Because G is an r by s matrix, k is bounded by the number of links s. If the Internet topology is a strict hierarchy like a tree, $s = O(n)$, thus $k = O(n)$. But if there is no hierarchy at all (*e.g.* a clique), $k = O(n^2)$ because all the $O(n^2)$ paths are linearly independent. Tangmunarunkit *et al.* found that the power-law degree Internet topology has moderate hierarchy [22]. It is our conjecture that $k = O(n \log n)$.

In this section, we will show through linear regression on both synthetic and real topologies that k is indeed bounded by $O(n \log n)$ for reasonably large n (*e.g*, 100). We explain it based on the power-law degree distribution of the Internet topology and the AS (Autonomous System) hierarchy.

We experiment with three types of BRITE [24] router-level topologies - Barabasi-Albert, Waxman and hierarchical models - as well as with a real router topology with 284,805 nodes [25]. For hierarchical topologies, BRITE first generates an autonomous system (AS) level topology with a Barabasi-Albert model or a Waxman model. Then for each AS, BRITE generates the router-level topologies with another Barabasi-Albert model or Waxman model. So there are four types of possible topologies. We show one of them as an example because they all have similar trends (see [2] for complete results).

We randomly select end hosts which have the least degree (*i.e.*, leaf nodes) to form an overlay network. We test by linear regression of k on $O(n)$, $O(n \log n)$, $O(n^{1.25})$, $O(n^{1.5})$, and $O(n^{1.75})$. As shown in Fig. 4, results for each type of topology are averaged over three runs with different topologies for synthetic ones and with different random sets of end hosts for the real one. We find that for Barabasi-Albert, Waxman and real topologies, $O(n)$ regression has the least residual errors - actually k even grows slower than $O(n)$. The hierarchical models have higher k, and most of them have $O(n \log n)$ as the best fit. Conservatively speaking, we have $k = O(n \log n)$.
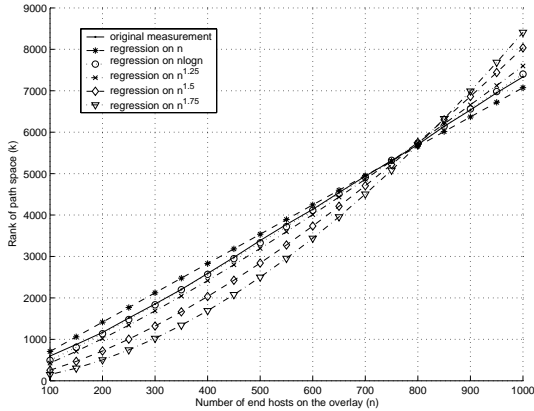
Note that such trend still holds when the end hosts are sparsely distributed in the Internet, *e.g.*, when each end host is in a different access network. One extreme case is the "star" topology - each end host is connected to the same center router via its own access network. In such a topology, there are only n links. Thus $k = O(n)$. Only topologies with very dense connectivity, like a full clique, have $k = O(n^2)$. Those topologies have little link sharing among the end-to-end paths.

The key observation is that when n is sufficiently large, such dense connectivity is very unlikely to exist in the Internet because of the power-law degree distribution. Tangmunarunkit *et al.* found that link usage, as measured by the set of node pairs (source-destination pairs) whose traffic traverses the link, also follows a power-law distribution, *i.e.*, there is a very small number of links that are on the shortest paths of the majority of node pairs. So there is significant amount of link sharing among the paths, especially for backbone links, customer links, and peering links.

Such link sharing can easily lead to rank deficiency of the path matrix for overlay networks. As an example, consider an overlay within a single AS. The AS with the largest number of links (exclusive of customer and peering links) in [26]
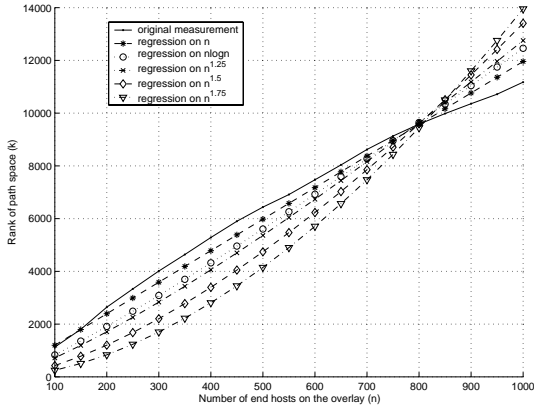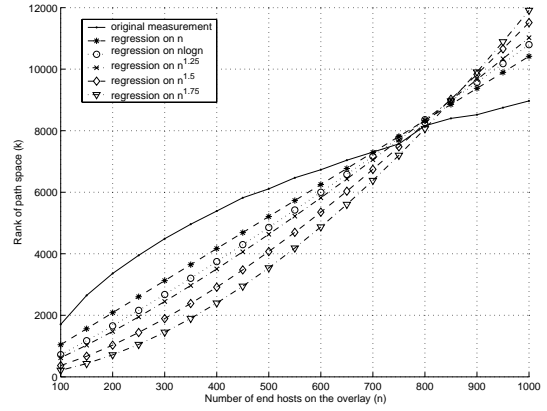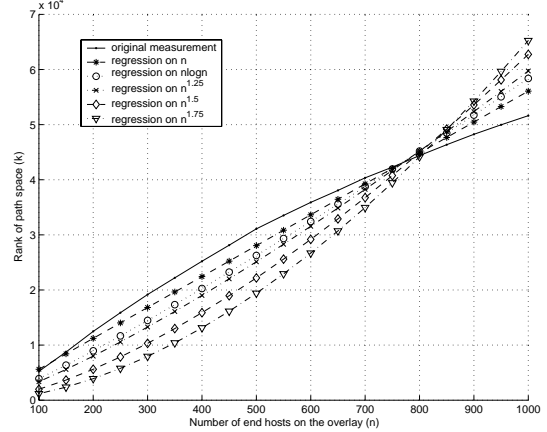
Barabasi-Albert model of 20K nodes

Waxman model of 10K nodes

Hierarchical model of 20K nodes
(AS-level: Barabasi-Albert and router level: Waxman)

A real topology of 284,805 routers

Figure 4: Regression of k in various functions of n under different router-level topologies.

has 5,300 links. Even considering the coverage factor (55.6% as in Table 2 of [26]), there are at most 9,600 links. Since there are $n(n-1)$ paths among n nodes, link sharing must occur before $n = 100$; in fact, substantial link sharing is likely to occur for even smaller n.

Now consider an overlay network that spans two ASes connected by y customer/peering links, with $n/2$ nodes in one AS and $n/2$ nodes in the other. The $n^2/2$ cross-AS paths can be modelled as linear combination of $2y \times n + 2y$ virtual links - bi-directional links from each end host to its y peering link routers, and y bi-directional peering links. Thus given y is normally much less than n and can be viewed as a constant, only $O(n)$ paths need to be measured for the $O(n^2)$ cross-AS paths.

Now consider an overlay on multiple ASes. According to [27], there are only 20 ASes (*tier-1* providers) which form the dense core of the Internet. These ASes are connected almost as a clique, while the rest of the ASes have far less dense peering connectivity. So when the size of an overlay is reasonably big (*e.g.*, $n > 100$), the number of customer and peering links that cross-AS paths traverse tends to grow much slower than $O(n^2)$. For example, a joining end host may only add one customer link to the overlay topology, and share the peering links that have been used by other end hosts. Meanwhile, only a few nodes are needed in a single AS before link sharing occurs in paths within an AS.

We believe this heavy sharing accounts for our empirical observation that $k = O(n)$ in a real router-level topology, and k grows at worst like $O(n \log n)$ in several generated topologies. Note that the real 284,805-router topology repre-

sents a fairly complete transit portion of the Internet [25]. In our analysis, we conservatively assume that there is only one end host connecting to each edge router to reduce the possible path sharing, but we still find $k = O(n)$ when $n > 100$.

5. DYNAMIC ALGORITHMS FOR TOPOLOGY CHANGES

During normal operation, new links may appear or disappear, routing paths between end hosts may change, and hosts may enter or exit the overlay network. These changes may cause rows or columns to be added to or removed from G, or entries in G may change. In this section, we design efficient algorithms to incrementally adapt to these changes.

5.1 Path Additions and Deletions

The basic building blocks for topology updates are path additions and deletions. We have already handled path additions in Algorithm 1; adding a path v during an update is no different than adding a path v during the initial scan of G. In both cases, we decide whether to add v to $\bar{G}$ and update R.

To delete a path that is not in $\bar{G}$ is trivial; we just remove it from G. But to remove a path from $\bar{G}$ is more complicated. We need to update R; this can be done in $O(k^2)$ time by standard algorithms (see e.g. Algorithm 3.4 in [28, p.338]). In general, we may then need to replace the deleted path with another measurement path. Finding a replacement path, or deciding that no such path is needed, can be done by re-scanning the rows of G as in Algorithm 1; however, this would take time $O(rk^2)$.

```
   procedure DeletePath(v, G, Ḡ, R)
1  if deleted path v is measured then
2      j = index of v in Ḡ
3      y = ḠᵀR⁻¹R⁻ᵀeⱼ
4      Remove v from G and Ḡ
5      Update R (Algorithm 3.4 in [28, p.338])
6      r = Gy
7      if ∃ i such that rᵢ ≠ 0 then
8          Add the ith path from G to Ḡ (Algorithm 1,
           steps 2-6)
       end
   end
9  else Remove v from G
```

Algorithm 2: Path deletion algorithm

We now describe Algorithm 2 to delete a path v more efficiently. Suppose v corresponds to the ith row in $\bar{G}$ and the jth row in G, we define $\bar{G}' \in \mathbb{R}^{(k-1) \times s}$ as the measurement path matrix after deleting the ith row, and $G' \in \mathbb{R}^{(r-1) \times s}$ as the path matrix after removing the jth row. By deleting v from $\bar{G}$, we reduce the dimension of $\bar{G}$ from k to $k-1$. Intuitively, our algorithm works in the following two steps.

1. Find a vector y that only describes the direction removed by deleting the ith row of $\bar{G}$.

2. Test if the path space of G' is orthogonal to that direction, i.e., find whether there is any path $p \in G'$ that has a non-zero component on that direction. If not, no replacement path is needed. Otherwise, replace v with any of such path p, and update the QR decomposition.

Next, we describe how each step is implemented. To find y which is in the path space of $\bar{G}$ but not of $\bar{G}'$, we solve the linear system $\bar{G}y = e_i$, where e_i is the vector of all zeros except for a one in entry i. This system is similar to the linear system we solved to find x_G, and one solution is $y = \bar{G}^T R^{-1} R^{-T} e_i$.

Once we have computed y, we compute $r = G'y$, where G' is the updated G matrix. Because we chose y to make $\bar{G}'y = 0$, all the elements of r corresponding to selected rows are zero. Paths such that $r_j \neq 0$ are guaranteed to be independent of $\bar{G}'$, since if row j of G could be written as $w^T \bar{G}'$ for some w, then r_j would be $w^T \bar{G}'y = 0$. If all elements of r are zero, then y is a null vector for all of G'; in this case, the dimension k' of the row space of G' is $k-1$, and we do not need to replace the deleted measurement path. Otherwise, we can find any j such that $r_j \neq 0$ and add the jth path to $\bar{G}'$ to replace the deleted path.

Take the overlay network in Fig. 3 for example, suppose $\bar{G}$ is composed of the paths AB and BC, i.e., $\bar{G} = \begin{bmatrix} 1 & 1 & 0 \\ 1 & 1 & 1 \end{bmatrix}$.

Then we delete path BC, $\bar{G}' = \begin{bmatrix} 1 & 1 & 0 \end{bmatrix}^T$ and $G' = \begin{bmatrix} 1 & 1 & 0 \\ 0 & 0 & 1 \end{bmatrix}$.

Applying Algorithm 2, we have $y = \begin{bmatrix} 0 & 0 & 1 \end{bmatrix}^T$ and $r = \begin{bmatrix} 0 & 1 \end{bmatrix}^T$. Thus the second path in G', AC, should be added to $\bar{G}'$. If we visualize such path deletion in reference to the geometry of the linear system, the path space of G' remains as a plane in Fig. 3, but $\bar{G}'$ only has one dimension of the path space left, so we need to add AC to $\bar{G}'$.

When deleting a path used in $\bar{G}$, the factor R can be updated in $O(k^2)$ time. To find a replacement row, we need to compute a sparse matrix-vector product involving G, which takes $O(n^2 \times (\text{average path length}))$ operations. Since most routing paths are short, the dominant cost will typically be the update of R. Therefore, the complexity of Algorithm 2 is $O(k^2)$.

5.2 End Hosts Join/Leave the Overlay

To add an end host h, we use Algorithm 1 to scan all the new paths from h, for a cost of $O(nk^2)$. However, it is inefficient to delete an end host h by directly using Algorithm 2 to delete all affected paths. If Algorithm 2 is used to delete a path that starts/ends at h, often another path that starts/ends at h is chosen as a replacement – and soon deleted in turn. To avoid this behavior, we remove all these paths from G first, then use the updated G in Algorithm 2 to select replacements as needed during the removal of paths that start/end at h. Each path in $\bar{G}$ can be removed in $O(k^2)$ time; the worst-case total cost of end host deletion is then $O(nk^2)$.

5.3 Routing Changes

In the network, routing changes or link failures can affect multiple paths in G. Previous studies have shown that end-to-end Internet paths generally tend to be stable for significant lengths of time, e.g., for at least a day [29, 30]. So we can incrementally measure the topology to detect changes. Each end host measures the paths to all other end hosts daily, and for each end host, such measurement load can be evenly distributed throughout the day. In addition to the periodic route measurement, if any path is found to have large loss rate changes, we will check its route instantly.

For each link, we keep a list of the paths that traverse it. If any path is reported as changed for certain link(s), we will examine all other paths that go through those link(s) because it is highly likely that those paths can change their routes as well. We use Algorithms 1 and 2 to incrementally incorporate each path change.

Unlike $O(n^2)$ approaches (e.g., RON), we need some extra traceroute measurement. However, the key point is that the end-to-end routing remains much more stable than its loss rate, thus requires far less frequent measurement. So the savings on loss rate probing dwarf the traceroute overhead.

6. LOAD BALANCING AND TOPOLOGY ERROR HANDLING

To further improve the scalability and accuracy, we need to have good load balancing and handle topology measurement errors, as discussed in this section.

6.1 Measurement Load Balancing

To avoid overloading any single node or its access link, we evenly distribute the measurements among the end hosts. We randomly reorder the paths in G before scanning them for selection in Algorithm 1. Since each path has equal probability of being selected for monitoring, the measurement load on each end host is similar. Note any basis set generated from Algorithm 1 is sufficient to describe all paths G. Thus the load balancing has no effect on the loss rate estimation accuracy.

6.2 Handling Topology Measurement Errors

As our goal is to estimate the end-to-end path loss rate instead of any interior link loss rate, we can tolerate certain topology measurement inaccuracies, such as incomplete routing information and poor router alias resolution.

For completely untraceable paths, we add a direct link between the source and the destination. In our system, these paths will become selected paths for monitoring. For paths with incomplete routing information, we add links from where the normal route becomes unavailable (*e.g.*, self loops or displaying "* * *" in traceroute), to where the normal route resumes or to the destination if such anomalies persist until the end. For instance, if the measured route is $(src, ip_1, "* * *", ip_2, dest)$, the path is composed of three links: $(src\ ip_1)$, (ip_1, ip_2), and $(ip_2, dest)$. By treating the untraceable path (segment) as a normal link, the resulting topology is equivalent to the one with complete routing information for calculating the path loss rates.

For topologies with router aliases presenting one physical link as several links, we have little need to resolve these aliases. At worst, our failure to recognize the links as the same will result in a few more path measurements because the rank of G will be higher. For these links, their corresponding entries in x_G will be assigned similar values because they are actually a single link. Thus the path loss rate estimation accuracy is not affected, as verified by Internet experiments in Sec. 8. In addition, our system is robust to measurement node failures and node changes by providing bounds on the estimated loss rates.

7. EVALUATION

In this section, we present our evaluation metrics, simulation methodology and simulation results.

7.1 Metrics

The metrics include path loss rate estimation accuracy, variation of measurement loads among the end hosts, and speed of setup, update, and topology change adaptation.

To compare the inferred loss rate $\hat{p}$ with real loss rate p, we analyze both absolute error and error factor. The absolute error is $|p - \hat{p}|$. We adopt the error factor $F_\varepsilon(p, \hat{p})$ defined in [9] as follows:

$$F_\varepsilon(p, \hat{p}) = \max\left\{ \frac{p(\varepsilon)}{\hat{p}(\varepsilon)}, \frac{\hat{p}(\varepsilon)}{p(\varepsilon)} \right\} \qquad (7)$$

where $p(\varepsilon) = \max(\varepsilon, p)$ and $\hat{p}(\varepsilon) = \max(\varepsilon, \hat{p})$. Thus, p and $\hat{p}$ are treated as no less than ε, and then the error factor is the maximum ratio, upwards or downwards, by which they differ. We use the default value $\varepsilon = 0.001$ as in [9]. If the estimation is perfect, the error factor is one.

Furthermore, we classify a path to be lossy if its loss rate exceeds 5%, which is the threshold between "tolerable loss" and "serious loss" as defined in [20]. We report the true number of lossy paths, the percentage of real lossy paths identified (coverage) and the false positive rate, all averaged over five runs of experiment for each configuration.

There are two types of measurement load: 1) sending probes, and 2) receiving probes and computing loss rates. The load reflects the CPU and uplink/downlink bandwidth consumption. For each end host h, its measurement load is linearly proportional to, and thus denoted by the number of monitored paths with h as sender/receiver. Then we compute its variation across end hosts in terms of the *coefficient of variation* (CV) and the *maximum vs. mean ratio* (MMR), for sending load and receiving load separately. The CV of a distribution x, defined as below, is a standard metric for measuring inequality of x, while the MMR checks if there is any single node whose load is significantly higher than the

average load.

$$CV(x) = \frac{standard\ deviation(x)}{mean(x)} \qquad (8)$$

The simulations only consider undirected links, so for each monitored path, we randomly select one end host as sender and the other as receiver. This is applied to all simulations with or without load balancing.

7.2 Simulation Methodology

We consider the following dimensions for simulation.

- Topology type: three types of synthetic topologies from BRITE (see Sec. 7.3) and a real router-level topology from [25]. All the hierarchical models have similar results, we just use Barabasi-Albert at the AS level and Waxman at the router level as the representative.

- Topology size: the number of nodes ranges from 1000 to 20000 [2]. Note that the node count includes both internal nodes (i.e., routers) and end hosts.

- Fraction of end hosts on the overlay network: we define end hosts to be the nodes with the least degree. Then we randomly choose from 10% to 50% of end hosts to be on the overlay network. This gives us pessimistic results because other distributions of end hosts will probably have more sharing of the routing paths among them. We prune the graphs to remove the nodes and links that are not referenced by any path on the overlay network.

- Link loss rate distribution: 90% of the links are classified as "good" and the rest as "bad". We use two different models for assigning loss rate to links as in [10]. In the first model ($LLRD_1$), the loss rate for good links is selected uniformly at random in the 0-1% range and that for bad links is chosen in the 5-10% range. In the second model ($LLRD_2$), the loss rate ranges for good and bad links are 0-1% and 1-100% respectively. Given space limitations, most results are under model $LLRD_1$ except for Sec. 7.4.

- Loss model: After assigning each link a loss rate, we use either a Bernoulli or a Gilbert model to simulate the loss processes at each link. For a Bernoulli model, each packet traversing a link is dropped at independently fixed probability as the loss rate of the link. For a Gilbert model, the link fluctuates between a good state (no packet dropped) and a bad state (all packets dropped). According to Paxon's observed measurement of Internet [31], the probability of remaining in bad state is set to be 35% as in [10]. Thus, the Gilbert model is more likely to generate bursty losses than the Bernoulli model. The other state transition probabilities are selected so that the average loss rates matches the loss rate assigned to the link.

We repeat our experiments five times for each simulation configuration unless denoted otherwise, where each repetition has a new topology and new loss rate assignments. The path loss rate is simulated based on the transmission of 10000 packets. Using the loss rates of selected paths as input, we compute x_G, then the loss rates of all other paths.

---

[2]20000 is the largest topology we can simulate on a 1.5GHz Pentium 4 machine with 512M memory.
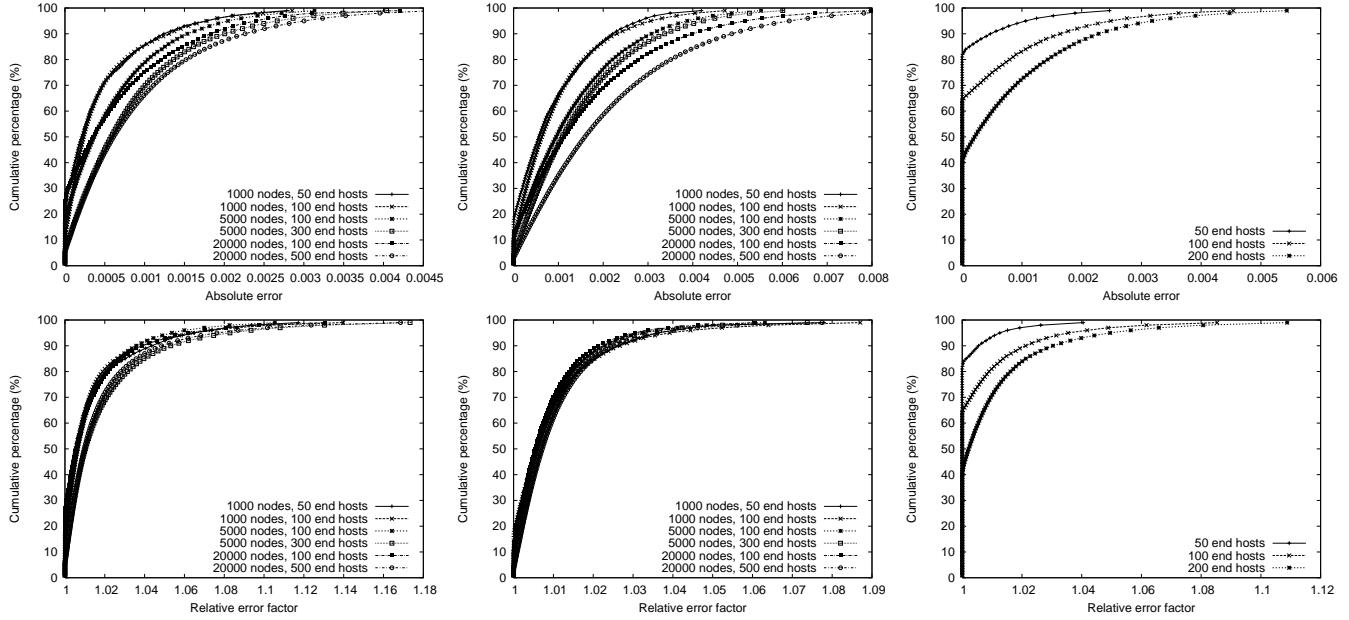
BRITE Barabasi-Albert topology   BRITE Hierarchical topology   Real topology of 284K routers

Figure 5: Cumulative distribution of absolute errors (top) and error factors (bottom) under Gilbert loss model for various topologies.

# of nodes	# of end hosts total	OL(n)	# of paths(r)	# of links original	AP	rank (k)	MPR (k/r)	lossy paths (Bernoulli) real	coverage	FP	lossy paths (Gilbert) real	coverage	FP
1000	506	50	1225	1997	443	275	22%	437	99.6%	1.3%	437	100.0%	0.2%
1000	506	100	4950	1997	791	543	11%	2073	99.0%	2.0%	1688	99.9%	0.2%
5000	2489	100	4950	9997	1615	929	19%	2271	99.1%	2.0%	2277	99.7%	0.1%
5000	2489	300	44850	9997	3797	2541	6%	19952	98.6%	4.1%	20009	99.6%	0.3%
20000	10003	100	4950	39997	2613	1318	27%	2738	98.4%	3.4%	2446	99.5%	0.6%
20000	10003	500	124750	39997	11245	6755	5%	67810	97.8%	5.5%	64733	99.5%	0.4%

# of nodes	# of end hosts total	OL(n)	# of paths(r)	# of links original	AP	rank (k)	MPR (k/r)	lossy paths (Bernoulli) real	coverage	FP	lossy paths (Gilbert) real	coverage	FP
1000	335	50	1225	2000	787	486	40%	704	99.0%	1.1%	579	99.6%	0.4%
1000	335	100	4950	2000	1238	909	18%	2544	98.5%	4.6%	2539	99.7%	0.5%
5000	1680	100	4950	10000	2996	1771	36%	3067	97.5%	3.9%	3024	99.5%	0.4%
5000	1680	300	44850	10000	6263	4563	10%	29135	96.8%	7.1%	28782	99.1%	1.1%
20000	6750	100	4950	40000	5438	2606	53%	3735	98.4%	2.3%	3607	99.6%	0.4%
20000	6750	500	124750	40000	20621	13769	11%	93049	96.1%	5.7%	92821	99.1%	1.5%

# of nodes	# of end hosts total	OL(n)	# of paths(r)	# of links original	AP	rank (k)	MPR (k/r)	lossy paths (Bernoulli) real	coverage	FP	lossy paths (Gilbert) real	coverage	FP
1000	312	50	1225	2017	441	216	18%	1034	98.8%	2.0%	960	99.6%	0.5%
1000	312	100	4950	2017	796	481	10%	4207	98.4%	1.6%	3979	99.6%	0.3%
5000	1608	100	4950	10047	1300	526	11%	4688	99.1%	0.6%	4633	99.8%	0.2%
5000	1608	300	44850	10047	3076	1787	4%	42331	99.2%	0.8%	42281	99.8%	0.1%
20000	6624	100	4950	40077	2034	613	12%	4847	99.8%	0.2%	4830	100.0%	0.1%
20000	6624	500	124750	40077	7460	3595	3%	122108	99.5%	0.3%	121935	99.9%	0.1%

# of end hosts on overlay (n)	# of paths(r)	# of links after pruning	rank (k)	MPR (k/r)	lossy paths (Bernoulli) real	coverage	FP	lossy paths (Gilbert) real	coverage	FP
50	1225	2098	1017	83%	891	99.7%	0.9%	912	100.0%	0.2%
100	4950	5413	3193	65%	3570	98.7%	1.9%	3651	99.6%	0.3%
200	19900	12218	8306	42%	14152	97.9%	3.1%	14493	99.6%	0.4%

Table 2: Simulation results for three types of BRITE router topologies: Barabasi-Albert (top), Waxman (upper middle) and hierarchical model (lower middle), and a real router topology of 284,805 nodes (bottom). OL gives the number of end hosts on the overlay network. AP shows the number of links after pruning (*i.e.*, remove the nodes and links that are not on the overlay paths). MPR (monitored path ratio) is the fraction of the total end-to-end paths which we monitor. FP is the false positive rate.

# of nodes	OL size (n)	Barabasi-Albert model								hierarchical model							
		CV				MMR				CV				MMR			
		sender		receiver		sender		receiver		sender		receiver		sender		receiver	
		LB	NLB	LB	NLB	LB	NLB	LB	NLB	LB	NLB	LB	NLB	LB	NLB	LB	NLB
1000	50	0.62	1.10	0.56	0.94	2.41	5.91	3.07	4.09	0.52	0.96	0.53	0.87	2.28	4.80	2.51	4.29
	100	0.61	1.42	0.64	1.34	3.21	11.33	3.61	10.67	0.51	1.38	0.47	1.39	2.74	10.06	2.32	10.27
5000	100	0.44	0.89	0.47	0.97	2.25	6.11	2.36	6.50	0.49	1.18	0.53	1.39	2.60	9.18	2.97	10.16
	300	0.52	1.59	0.51	1.51	2.97	18.70	2.74	17.25	0.47	1.72	0.48	1.76	3.47	23.93	4.13	25.76
20000	100	0.36	0.55	0.40	0.59	1.93	3.20	2.29	3.69	0.48	1.17	0.43	1.09	3.04	8.86	2.56	7.09
	500	0.52	1.36	0.53	1.35	2.64	19.21	3.01	16.82	0.46	1.85	0.46	1.89	5.01	25.85	5.56	27.67

Table 3: Measurement load (as sender or receiver) distribution for various BRITE topologies. OL Size is the number of end hosts on overlay. "LB" means with load balancing, and "NLB" means without load balancing.

7.3 Results for Different Topologies

For all topologies in Sec. 7.2, we achieve high loss rate estimation accuracy. Results for the Bernoulli and the Gilbert models are similar. Since the Gilbert loss model is more realistic, we plot the cumulative distribution functions (CDFs) of absolute errors and error factors with the Gilbert model in Fig. 5. For all the configurations, the absolute errors are less than 0.008 and the error factors are less than 1.18. Waxman topologies have similar results, and we omit them in the interest of space.

The lossy path inference results are shown in Table 2. Notice that k is much smaller than the number of IP links that the overlay network spans, which means that there are many IP links whose loss rates are unidentifiable. Although different topologies have similar asymptotic regression trend for k as $O(n \log n)$, they have different constants. For an overlay network with given number of end hosts, the more IP links it spans on, the bigger k is. We found that Waxman topologies have the largest k among all synthetic topologies. For all configurations, the lossy path coverage is more than 96% and the false positive ratio is less than 8%. Many of the false positives and false negatives are caused by small estimation errors for paths with loss rates near the 5% threshold.

We also test our algorithms in the 284,805-node real router-level topology from [25]. There are 65,801 end host routers and 860,683 links. We get the same trend of results as illustrated in Fig. 5 and Table 2. The CDFs include all the path estimates, including the monitored paths for which we know the real loss rates. Given the same number of end hosts, the ranks in the real topology are higher than those of the synthetic ones. But as we find in Sec. 4, the growth of k is still bounded by $O(n)$.

7.4 Results for Different Link Loss Rate Distribution and Running Time

We have also run all the simulations above with model $LLRD_2$. The loss rate estimation is a bit less accurate than it is under $LLRD_1$, but we still find over 95% of the lossy paths with a false positive rate under 10%. Given space limitations, we only show the lossy path inference with the Barabasi-Albert topology model and the Gilbert loss model in Table 4.

The running time for $LLRD_1$ and $LLRD_2$ are similar, as in Table 4. All speed results in this paper are based on a 1.5 GHz Pentium 4 machine with 512M memory. Note that it takes about 20 minutes to setup (select the measurement paths) for an overlay of 500 end hosts, but only several seconds for an overlay of size 100. The update (loss rate calculation) time is small for all cases, only 4.3 seconds for 124,750 paths. Thus it is feasible to update online.

# of nodes	end hosts		lossy paths (Gilbert)			speed (second)	
	total	OL	real	coverage	FP	setup	update
1000	506	50	495	99.8%	1.1%	0.13	0.08
		100	1989	99.8%	3.0%	0.91	0.17
5000	2489	100	2367	99.6%	3.5%	1.98	0.22
		300	21696	99.2%	1.4%	79.0	1.89
20000	10003	100	2686	98.8%	1.1%	3.00	0.25
		500	67817	99.0%	4.6%	1250	4.33

Table 4: Simulation results with model $LLRD_2$. Use the same Barabasi-Albert topologies as in Table 2. Refer to Table 2 for statistics like rank. FP is the false positive rate. OL means overlay network.

7.5 Results for Measurement Load Balancing

We examine the measurement load distribution for both synthetic and real topologies, and the results are shown in Table 3. Given the space constraints, we only show the results for Barabasi-Albert and hierarchical model. Our load balancing scheme reduces CV and MMR substantially for all cases, and especially for MMR. For instance, a 500-node overlay on a 20000-node network of Barabasi-Albert model has its MMR reduced by 7.3 times.

We further plot the histogram of measurement load distribution by putting the load values of each node into 10 equally spaced bins, and counting the number of nodes in each bin as y-axis. The x-axis denotes the center of each bin, as illustrated in Fig. 6. With load balancing, the histogram roughly follow the normal distribution. In contrast, the histogram without load balancing is close to an exponential distribution. Note that the y-axis in this plot is logarithmic: an empty bar means that the bin contains one member, and 0.1 means the bin is empty.

(a) with load balancing   (b) without load balancing
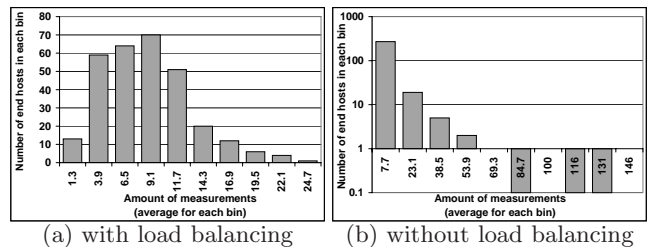
Figure 6: Histogram of the measurement load distribution (as sender) for an overlay of 300 end hosts on a 5000-node Barabasi-Albert topology.

7.6 Results for Topology Changes

We study two common scenarios in P2P and overlay networks: end hosts joining and leaving as well as routing changes. Again, the Bernoulli and the Gilbert models have similar results, thus we only show those of the Gilbert model.

7.6.1 End hosts join/leave

# of end hosts	# of paths	rank	lossy paths		
			real	coverage	FP
40	780	616	470	99.9%	0.2%
+5 (45)	+210 (990)	+221 (837)	+153 (623)	100.0%	0.1%
+5 (50)	+235 (1225)	+160 (997)	+172 (795)	99.8%	0.2%

Table 5: Simulation results for adding end hosts on a real router topology. FP is the false positive rate. Denoted as "+added_value (total_value)".

# of end hosts	# of paths	rank	lossy paths		
			real	coverage	FP
60	1770	1397.0	1180.3	99.9%	0.2%
-5 (55)	-285 (1485)	-245.3 (1151.7)	-210.0 (970.3)	99.8%	0.2%
-10 (50)	-260 (1225)	-156.7 (995.0)	-150.6 (819.7)	99.9%	0.1%

Table 6: Simulation results for deleting end hosts on a real router topology. FP is the false positive rate. Denoted as "-reduced_value (total_value)".

For the real router topology, we start with an overlay network of 40 random end hosts. Then we randomly add an end host to join the overlay, and repeat the process until the size of the overlay reaches 45 and 50. Averaged over three runs, the results in Table 5 show that there is no obvious accuracy degradation caused by accumulated numerical errors. The average running time for adding a path is 125 msec, and for adding a node, 1.18 second. Notice that we add a block of paths together to speedup adding node (Sec. 3.2).

Similarly, for removing end hosts, we start with an overlay network of 60 random end hosts, then randomly select an end host to delete from the overlay, and repeat the process until the size of the overlay is reduced to 55 and 50. Again, the accumulated numerical error is negligible as shown in Table 6. As shown in Sec. 5, deleting a path in $\bar{G}$ is much more complicated than adding a path. With the same machine, the average time for deleting a path is 445 msec, and for deleting a node, 16.9 seconds. We note that the current implementation is not optimized: we can speed up node deletion by processing several paths simultaneously, and we can speed up path addition and deletion with iterative methods such as CGNE or GMRES [32]. Since the time to add/delete a path is $O(k^2)$, and to add/delete a node is $O(nk^2)$, we expect our updating scheme to be substantially faster than the $O(n^2k^2)$ cost of re-initialization for larger n.

7.6.2 Routing changes

# of paths affected	40.7
# of monitored paths affected	36.3
# of unique nodes affected	41.7
# of real lossy paths (before/after)	761.0/784.0
coverage (before/after)	99.8%/99.8%
false positive rate (before/after)	0.2%/0.1%
average running time	17.3 seconds

Table 7: Simulation results for removing a link from a real router topology.

We form an overlay network with 50 random end hosts on the real router topology. Then we simulate topology changes by randomly choosing a link that is on some path of the overlay and removing of such a link will not cause disconnection for any pair of overlay end hosts. Then we assume that the link is broken, and re-route the affected path(s). Algorithms in Sec. 5 incrementally incorporate each path change. Averaged over three runs, results in Table 7 show that we adapt quickly, and still have accurate path loss rate estimation.

We also simulate the topology changes by adding a random link on some path(s) of the overlay. The results are similar as above, so we omit them here for brevity.

8. INTERNET EXPERIMENTS

8.1 Methodology

We implemented our system on the PlanetLab [33] testbed, and deployed it on 51 PlanetLab hosts, each from a different organization as shown in Table 8. All the international PlanetLab hosts are universities.

Areas and Domains			# of hosts
US (40)	.edu		33
	.org		3
	.net		2
	.gov		1
	.us		1
International (11)	Europe (6)	France	1
		Sweden	1
		Denmark	1
		Germany	1
		UK	2
	Asia (2)	Taiwan	1
		Hong Kong	1
	Canada		2
	Australia		1

Table 8: Distribution of selected PlanetLab hosts.

First, we measure the topology among these sites by simultaneously running "traceroute" to find the paths from each host to all others. Each host saves its destination IP addresses for sending measurement packets later. Then we measure the loss rates between every pair of hosts. Our measurement consists of 300 trials, each of which lasts 300 msec. During a trial, each host sends a 40-byte UDP packet [3] to every other host. Usually the hosts will finish sending before the 300 msec trial is finished. For each path, the receiver counts the number of packets received out of 300 to calculate the loss rate.

To prevent any host from receiving too many packets simultaneously, each host sends packets to other hosts in a different random order. Furthermore, any single host uses a different permutation in each trial so that each destination has equal opportunity to be sent later in each trial. This is because when sending packets in a batch, the packets sent later are more likely to be dropped. Such random permutations are pre-generated by each host. To ensure that all hosts in the network take measurements at the same time, we set up sender and receiver daemons, then use a well-connected server to broadcast a "START" command.

Will the probing traffic itself cause losses? We performed sensitivity analysis on sending frequency as shown in Fig. 7.

---

[3]20-byte IP header + 8-byte UDP header + 12-byte data on sequence number and sending time.

All experiments were executed between 1am-3am PDT June 24, 2003, when most networks are free. The traffic rate from or to each host is $(51 - 1) \times sending\_freq \times 40$ bytes/sec. The number of lossy paths does not change much when the sending rate varies, except when the sending rate is over 12.8Mbps, since many servers can not sustain that sending rate. We choose a 300 msec sending interval to balance quick loss rate statistics collection with moderate bandwidth consumption.
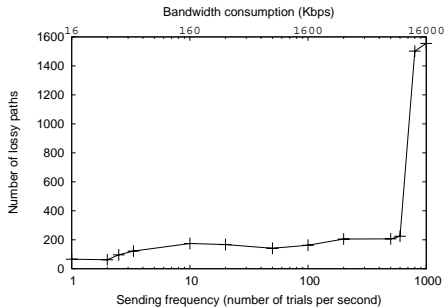

Figure 7: Sensitivity test of sending frequency

Note that the experiments above use $O(n^2)$ measurements so that we can compare the real loss rates with our inferred loss rates. In fact, our technique only requires $O(n \log n)$ measurements. Thus, given good load balancing, each host only needs to send to $O(\log n)$ hosts. In fact, we achieve similar CV and MMR for measurement load distribution as in the simulation. Even for an overlay network of 400 end hosts on the 284K-node real topology used before, k = 18668. If we reduce the measurement frequency to one trial per second, the traffic consumption for each host is $18668/400 \times 40$ bytes/sec = 14.9Kbps, which is typically less than 5% of the bandwidth of today's "broadband" Internet links. We can use adaptive measurement techniques in [3] to further reduce the overheads.

loss rate	[0, 0.05)	lossy path [0.05, 1.0] (4.1%)				
		[0.05, 0.1)	[0.1, 0.3)	[0.3, 0.5)	[0.5, 1.0)	1.0
%	95.9%	15.2%	31.0%	23.9%	4.3%	25.6%

Table 9: Loss rate distribution: lossy vs. non-lossy and the sub-percentage of lossy paths.

8.2 Results

From June 24 to June 27, 2003, we ran the experiments 100 times, mostly during peak hours 9am - 6pm PDT. Each experiment generates $51 \times 50 \times 300 = 765K$ UDP packets, totaling 76.5M packets for all experiments. We run the loss rate measurements three to four times every hour, and run the pair-wise traceroute every two hours. Across the 100 runs, the average number of selected monitoring paths ($\bar{G}$) is 871.9, about one third of total number of end-to-end paths, 2550. Table 9 shows the loss rate distribution on all the paths of the 100 runs. About 96% of the paths are non-lossy. Among the lossy paths, most of the loss rates are less than 0.5. Though we try to choose stable nodes for experiments, about 25% of the lossy paths have 100% losses and are likely caused by node failures or other reachability problems as discussed in Sec. 8.2.2.

8.2.1 Accuracy and speed

When identifying the lossy paths (loss rates > 0.05), the average coverage is 95.6% and the average false positive rate is 2.75%. Fig. 8 shows the CDFs for the coverage and the

false positive rate. Notice that 40 runs have 100% coverage and 90 runs have coverage over 85%. 58 runs have no false positives and 90 runs have false positive rates less than 10%.
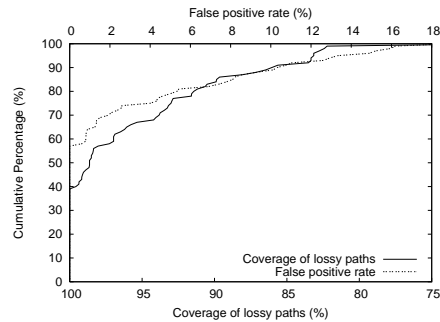

Figure 8: Cumulative percentage of the coverage and the false positive rates for lossy path inference in the 100 experiments.

As in the simulations, many of the false positives and false negatives are caused by the 5% threshold boundary effect. The average absolute error across the 100 runs is only 0.0027 for all paths, and 0.0058 for lossy paths. We pick the run with the worst accuracy in coverage (69.2%), and plot the CDFs of absolute errors and error factors in Fig. 9. Since we only use 300 packets to measure the loss rate, the loss rate precision granularity is 0.0033, so we use $\varepsilon = 0.005$ for error factor calculation. The average error factor is only 1.1 for all paths.
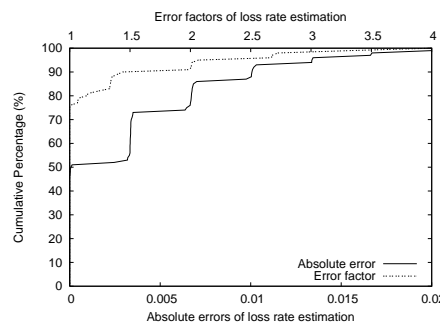

Figure 9: Cumulative percentage of the absolute errors and error factors for the experiment with the worst accuracy in coverage.

Even for the worst case, 95% of absolute errors in loss rate estimation are less than 0.014, and 95% of error factors are less than 2.1. To further view the overall statistics, we pick 95 percentile of absolute errors and error factors in each run, and plot the CDFs on those metrics. The results are shown in Fig. 10. Notice that 90 runs have the 95 percentile of absolute errors less than 0.0133, and 90 runs have the 95 percentile of error factors less than 2.0.

The average running time for selecting monitoring paths based on topology measurement is 0.75 second, and for loss rate calculation of all 2550 paths is 0.16 second.

8.2.2 Topology error handling

The limitation of traceroute, which we use to measure the topology among the end hosts, led to many topology measurement inaccuracies. As found in [34], many of the routers on the paths among PlanetLab nodes have aliases. We did not use sophisticated techniques to resolve these aliases. Thus, the topology we have is far from accurate. Furthermore, in the PlanetLab experiments, some nodes were down,
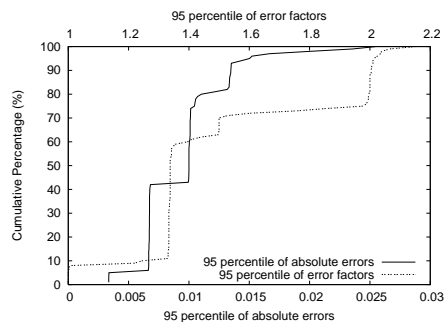
Figure 10: Cumulative percentage of the 95 percentile of absolute errors and error factors for the 100 experiments.

or were unreachable from certain nodes. Meanwhile, some routers are hidden and we only get partial routing paths. Averaging over 14 sets of traceroutes, 245 out of $51 \times 50 = 2550$ paths have no or incomplete routing information. The accurate loss rate estimation results show that our topology error handling is successful.

9. CONCLUSIONS

In this paper, we improve, implement and evaluate an algebraic approach [1] for adaptive scalable overlay network monitoring. For an overlay of n end hosts, we selectively monitor a basis set of $O(n \log n)$ paths which can fully describe all the $O(n^2)$ paths. Then the measurements of the basis set are used to infer the loss rates of all other paths. Our approach works in real time, offers fast adaptation to topology changes, distributes balanced load to end hosts, and handles topology measurement errors. Both simulation and real Internet implementation yield promising results.

For even more efficient monitored path selection, we plan to investigate the use of iterative methods [32], [35] both to select rows and to compute loss rate vectors. In our preliminary experiments, the path matrix G has been well-conditioned, which suggests that iterative methods may converge quickly.

10. ACKNOWLEDGEMENT

11. REFERENCES

[1] Y. Chen, D. Bindel, and R. H. Katz, "Tomography-based overlay network monitoring," in *ACM SIGCOMM Internet Measurement Conference (IMC)*, 2003.

[2] Y. Chen, *Towards a Scalable, Adaptive and Network-aware Content Distribution Network*, Ph.D. thesis, University of California at Berkeley, Nov. 2003.

[3] D. G. Andersen et al., "Resilient overlay networks," in *Proc. of ACM SOSP*, 2001.

[4] T. S. E. Ng and H. Zhang, "Predicting Internet network distance with coordinates-based approaches," in *Proc.of IEEE INFOCOM*, 2002.

[5] S. Ratnasamy et al., "Topologically-aware overlay construction and server selection," in *Proc. of IEEE INFOCOM*, 2002.

[6] P. Francis et al., "IDMaps: A global Internet host distance estimation service," *IEEE/ACM Trans. on Networking*, Oct. 2001.

[7] Y. Chen et al., "On the stability of network distance estimation," in *ACM SIGMETRICS Performance Evaluation Review (PER)*, Sep. 2002.

[8] Mark Coates, Alfred Hero, Robert Nowak, and Bin Yu, "Internet Tomography," *IEEE Signal Processing Magazine*, vol. 19, no. 3, pp. 47–65, 2002.

[9] T. Bu, N. Duffield, F. Presti, and D. Towsley, "Network tomography on general topologies," in *ACM SIGMETRICS*, 2002.

[10] V. Padmanabhan, L. Qiu, and H. Wang, "Server-based inference of Internet link lossiness," in *IEEE INFOCOM*, 2003.

[11] D. Rubenstein, J. F. Kurose, and D. F. Towsley, "Detecting shared congestion of flows via end-to-end measurement," *ACM Transactions on Networking*, vol. 10, no. 3, 2002.

[12] Y. Shavitt, X. Sun, A. Wool, and B. Yener, "Computing the unmeasured: An algebraic approach to Internet mapping," in *IEEE INFOCOM*, 2001.

[13] H. C. Ozmutlu et al., "Managing end-to-end network performance via optimized monitoring strategies," *Journal of Network and System Management*, vol. 10, no. 1, 2002.

[14] C. Tang and P. McKinley, "On the cost-quality tradeoff in topology-aware overlay path probing," in *IEEE ICNP*, 2003.

[15] R. Caceres, N. Duffield, J. Horowitz, and D. Towsley, "Multicast-based inference of network-internal loss characteristics," *IEEE Transactions in Information Theory*, vol. 45, 1999.

[16] S. Floyd and V. Jacobson, "Random early detection gateways for congestion avoidance," *IEEE/ACM Transactions on Networking*, vol. 1, no. 4, 1993.

[17] N. Duffield et al., "Multicast-based loss inference with missing data," *IEEE Journal of Selected Areas of Communications*, vol. 20, no. 4, 2002.

[18] G.H. Golub and C.F. Van Loan, *Matrix Computations*, The Johns Hopkins University Press, 1989.

[19] E. Anderson et al., *LAPACK Users' Guide*, Society for Industrial and Applied Mathematics, Philadelphia, PA, third edition, 1999.

[20] Y. Zhang et al., "On the constancy of Internet path properties," in *Proc. of SIGCOMM IMW*, 2001.

[21] J.W. Demmel, *Applied Numerical Linear Algebra*, SIAM, 1997.

[22] H. Tangmunarunkit et al., "Network topology generators: Degree-based vs structural," in *ACM SIGCOMM*, 2002.

[23] M. Faloutsos, P. Faloutsos, and C. Faloutsos, "On power-law relationship of the Internet topology," in *ACM SIGCOMM*, 1999.

[24] A. Medina, I. Matta, and J. Byers, "On the origin of power laws in Internet topologies," in *ACM Computer Communication Review*, Apr. 2000.

[25] R. Govindan and H. Tangmunarunkit, "Heuristics for Internet map discovery," in *IEEE INFOCOM*, 2000.

[26] N. Spring, R. Mahajan, and D. Wetherall, "Measuring isp topologies with rocketfuel," in *ACM SIGCOMM*, 2002.

[27] L. Subrmanian, S. Agarwal, J. Rexford, and R. H.Katz, "Characterizing the Internet hierarchy from multiple vantage points," in *IEEE INFOCOM*, 2002.

[28] G. W. Stewart, *Matrix Algorithms: Basic Decompositions*, Society for Industrial and Applied Mathematics, 1998.

[29] V. Paxon, "End-to-end routing behavior in the Internet," *IEEE/ACM Transactions on Networking*, vol. 5, no. 5, 1997.

[30] Y. Zhang, V. Paxson, and S. Shenker, "The stationarity of Internet path properties: Routing, loss, and throughput," ACIRI Technical Report, May, 2000.

[31] V. Paxon, "End-to-end Internet packet dynamics," in *ACM SIGCOMM*, 1997.

[32] R. Barrett et al., *Templates for the Solution of Linear Systems: Building Blocks for Iterative Methods, 2nd Edition*, SIAM, Philadelphia, PA, 1994.

[33] PlanetLab, "http://www.planet-lab.org/," .

[34] N. Spring, D. Wetherall, and T. Anderson, "Scriptroute: A facility for distributed internet measurement," in *USITS*, 2003.

[35] C. Meyer and D. Pierce, "Steps toward an iterative rank-revealing method," Tech. Rep. ISSTECH-95-013, Boeing Information and Support Services, 1995.